Available online at www.sciencedirect.com

Journal of Applied Research and Technology

Journal of Applied Research and Technology 14 (2016) 425–433

www.jart.ccadet.unam.mx

Original

Application of poly(aspartic acid-citric acid) copolymer compound inhibitor as an effective and environmental agent against calcium phosphate in cooling water systems

Yu-ling Zhang *, Cai-xia Zhao, Xiao-dong Liu, Wei Li, Jiao-long Wang, Zhi-guang Hu

School of Environmental Science & Engineering, North China Electric Power University (NCEPU), Baoding, China

Received 3 May 2016; Received in revised form 18 July 2016; accepted 23 August 2016
Available online 1 December 2016

Abstract

Poly(aspartic acid-citric acid) copolymer (PAC) is a new product of poly(carboxylic acid) scale inhibitor. The study aims to develop a "green" water treatment agent for calcium phosphate scale. The article compares the efficiency of three polymeric antiscalants, poly(aspartic acid-citric acid) copolymer (PAC), polymaleic acid (HPMA) and a compound inhibitor (PAC-HPMA), for calcium phosphate scale prevention under varying experimental conditions. Inhibitor concentration, calcium concentration, system pH, temperature and experimental time were varied to determine their influences on inhibitor performance by the static scale inhibition method. The copolymer (PAC) was characterized by FTIR, ^{1}H NMR and ^{13}C NMR. The compound inhibitor was applied in the actual circulating cooling water system. An atomic force microscope (AFM), X-ray powder diffraction (XRD) and a scale formation process analysis were used to explore the scale inhibition mechanism. The results showed that scale inhibition rates of PAC, HPMA and PAC-HPMA against $Ca_3(PO_4)_2$ were, respectively, about 23%, 41.5% and 63% when the dosage was 8 mg/L in the experiment. The compound inhibitor showed the better inhibition performance than the above two kinds of monomers. Under the actual working conditions, the inhibition rate of compound inhibitor was close to 100% and completely met the actual application requirements of scale inhibitor in circulating cooling water systems. The main inhibition mechanism was the decomposition-chelation dispersion effect. The compound inhibitor can be used as an efficient "green" scale inhibitor for calcium phosphate.

Keywords: Poly(aspartic acid-citric acid) copolymer (PAC); Polymaleic acid (HPMA); Compound inhibitor (PAC-HPMA); Calcium phosphate; Inhibition rate

1. Introduction

Phosphorus scale inhibitors can prevent the formation of calcium carbonate and calcium sulfate scales; however, the phosphorous-based compounds, particularly the poly(phosphate)s, may produce orthophosphate in hydrolysis reactions and exacerbate phosphate scaling when water contains significant hardness (Snoeyink & Jenkins, 1980). Phosphorus-based inhibitors, which can serve as nutrients leading to eutrification difficulties. Phosphorus and heavy-metal discharges are regulated in many areas of the world, and permissible limits are decreasing (Hasson, Shemer, & Sher, 2011). Furthermore, reclaimed water widely used in the circulating cooling system usually contains trace amounts of phosphorus compounds, such as orthophosphates, poly(phosphate)s and organophosphates, which cannot be completely removed from raw wastewater by secondary or advanced treatment (Wang, Wang, & Hou, 2016) and may increase calcium phosphate deposition in the circulating cooling system. Moreover, increasing cooling systems are operating under the larger cycles at the higher temperatures, so $Ca_3(PO_4)_2$ scale has become common in cooling water systems (Feng et al., 2014).

The growth of calcium phosphate scale in industrial processes causes serious problems. Especially, calcium phosphate scale deposited on heat exchanger surfaces in industrial cooling water systems, boiler, oil and gas production, geothermal energy and distillation systems, leads to overheating and thermal loss of

* Corresponding author.
E-mail address: zhangyuling_hit@163.com (Y.-l. Zhang).
Peer Review under the responsibility of Universidad Nacional Autónoma de México.

http://dx.doi.org/10.1016/j.jart.2016.08.006

systems (Wang, Shen, Li, & Wang, 2014). Undesirable scale deposits often cause numerous technical and economic problems (Belarbi, Gamby, Makhloufi, Sotta, & Tribollet, 2014). Calcium scaling from cooling water seriously affects the operation of recirculating cooling water facilities (Wang et al., 2014).

To prevent or minimize unfavorable events caused by scaling problems, it is necessary to add large quantities of scale inhibitors into cooling water systems (Lin & Singer, 2005; Zuhl & Amjad, 2010). Some polymers as scale inhibitors were synthesized to explore its inhibition effect. Zhang, Wang, Jin, and Zhu (2013) synthesized a polysaccharide sulfonate salt from a hetero-polysaccharide extracted from abandoned corn stalks and its scale inhibition rates against $CaSO_4$ and $Ca_3(PO_4)_2$ respectively reached 95% and 55%. Biodegradable polymers such as PASP and polyepoxysuccinic acid (PESA) have drawn much attention recently in view of environmental benefits (Liu, Dong, Li, Hui, & Lédion, 2012; Roweton, Huang, & Swift, 1997). Demadis and Stathoulopoulou (2006) reported that CMI, at a dosage of 4–6 mg/L, showed good inhibitory performance with regard to $CaCO_3$ and $CaSO_4$ scale formation. These polymers had the better anti-scaling performance for $CaCO_3$ and $CaSO_4$; nonetheless, their scale inhibition rate to $Ca_3(PO_4)_2$ was not outstanding, thus limiting their large-scale commercial applications (Xu, Zhang, Zhao, & Cui, 2013). Hence, it is necessary to develop environmentally friendly agent as efficient calcium phosphate scale inhibitor.

In the study, we firstly composited the compound inhibitor (PAC-HPMA) with aspartic acid-citric acid copolymer (PAC) and polymaleic acid (HPMA) according to a certain proportion. Then, following the static scale inhibition method, we compared the anti-scaling performances of PAC, HPMA, and PAC-HPMA with $Ca_3(PO_4)_2$ scale as the target and under different conditions (scale inhibitor dosage, pH, Ca^{2+} concentration, constant temperature and time). In addition, the compound inhibitor was applied in the actual circulating cooling water system. Atomic force microscope (AFM), X-ray powder diffraction (XRD) and scale formation process analysis were used to explore the scale inhibition mechanism.

2. Experimental

2.1. Reagents and instruments

HPMA (active component of 48%) was purchased from Taihe Chemical Reagent Co. Ltd. (Shandong, P.R. China). Poly(aspartic acid-citric acid) copolymer (PAC, *Mw*: 16,242; *Mn*: 11,255; PDI: 1.44; mole ratio of aspartic acid and citric acid is 9:1) and compound inhibitor (PAC-HPMA) were self-made in the laboratory.

Instruments used in the study included HH-S6 Digital constant temperature water bath pot, TP-214 electronic balance, UV-6000 PC spectrophotometer, CSPM5500 Perkin Elmer Spectrum 100 spectrometer (IR), Bruker Advance AV 50 MHz nuclear magnetic resonance spectrometer (NMR), atomic force microscope (AFM), and D8 Advance X-ray powder diffraction (XRD).

2.2. Synthesis and purification methods of PAC

The synthesis method was as follows: a certain amount of aspartic acid and citric acid were fully mixed. NaH_2PO_4 as catalyst and propylene carbonate (PC) as organic solvent were added into the above mixture to obtain suspension. The suspension reacted several minutes under microwave radiation to generate yellow fluffy product PSID called as intermediate. PSID was fully hydrolyzed by adding an appropriate amount of 6 mol/L NaOH solution. The color of the solution after hydrolyzation turned into red brown. The pH was adjusted to 3.84 by using hydrochloric acid, and then excess anhydrous ethanol was added into the solution. The object product (PAC) was obtained after filtering, drying and grinding.

Purification of PAC: excess anhydrous ethanol was added into 70% PAC solution to obtain the suspension. Then suspension was static settling for 30 min and the deposit was observed. After filtering, the deposit was added to excess anhydrous ethanol again. The above operation was repeated four times. High-purity PAC was gained after filtering, drying and grinding.

2.3. Determination of scale inhibition rate

$Ca_3(PO_4)_2$ inhibition tests were determined by the static scale inhibition method. According to the national standard of P.R. China concerning the code for the design of industrial circulating cooling water treatment (GB/T 22626-2008), after pH was adjusted to 9.0 using 1.0 g/L $Na_2B_4O_7{\cdot}10H_2O$, the testing solution containing 100 mg/L $CaCl_2$, 5 mg/L KH_2PO_4 and a certain amount of inhibitor was incubated at 80 °C for 10 h in water bath. The hot solution was filtered and the PO_4^{3-} concentration in the filtrate was detected by the ammonium molybdate spectrophotometric method. The inhibition rate of the scale inhibitor against $Ca_3(PO_4)_2$ scales was calculated according to Eq. (1):

$$\eta_{Ca_3(PO_4)_2} = \frac{\rho_1 - \rho_0}{\rho_2 - \rho_0} \times 100 \quad (1)$$

where ρ_1 and ρ_0 are the concentration of PO_4^{3-} in the supernatant after10 h test period in the presence and absence of the inhibitor, respectively; ρ_2 is the mass absorbance of all in to-be-tested solution.

2.4. Characterization of PAC

2.4.1. FTIR analysis

A small amount of purified samples were dried to constant weight in an oven at 60 °C, which were mixed with KBr and pressed onto disk. FTIR spectra in the range 400–4000 cm^{-1} of the copolymers were recorded by means of a Perkin Elmer Spectrum 100 spectrometer made in USA.

2.4.2. H NMR and ^{13}C NMR analysis

^{13}C NMR and ^{1}H NMR spectra of PAC were measured with a Bruker Advance AV 50 MHz NMR spectrometer made in Switzerland. 5 mg sample and 1 mL D_2O were used to measurement.

2.5. Atomic force microscope (AFM)

The solid samples were finely pretreated and placed on silicon wafers for atomic force microscope (AFM) analysis in tapping mode, of which the parameters were 1 Hz of scanning frequency, 1024 × 768 of resolution, and 0.8 for reference point.

2.6. X-ray powder diffraction (XRD)

XRD patterns were conducted by D8 Advance X-ray diffraction with a sealed ceramic tube X-ray source. Tube voltage and current were 40 kV and 50 mA, respectively. Wide-angle scanning was chosen with the other parameters as scan range from 5° to 90°, 4°/min for scanning speed and 0.02° for the step size.

3. Results and discussion

3.1. Characterization of PAC

3.1.1. FTIR analysis

Fig. 1 shows the FTIR spectra of the copolymer PAC. It is seen from the curve that the characteristic absorption peaks of N–H bond and C=O bond stretching vibration appear at the wave numbers of 3392.55 cm^{-1} and 1604.66 cm^{-1}, respectively. The peaks at around 911.75 cm^{-1} and 1298.22 cm^{-1} represent C–O of carboxyl stretching vibration and –OH out of plane deformation vibration, respectively. The absorption peaks at 1635.52 cm^{-1} and 526.53 cm^{-1} indicate the β structure of aspartic acid monomer polymerization. The band at 1074.28 cm^{-1} in Fig. 1 is caused by the bending vibration of $–CH_2–$ The FTIR analysis results showed that the function groups of copolymer had similar characteristics to those of PASP synthesized by thermal polymerization of aspartic acid, confirming the formation of PAC copolymer.

3.1.2. H NMR and ^{13}C NMR analysis

Fig. 2 shows the ^{13}C spectra of PAC copolymer. Contrast with related ^{13}C NMR spectrum chemical shift values, chemical shifts at 173.98 ppm, 172.46 ppm and 71.5 ppm appear carbonyl of acylamino, carbonyl and carbon of citric acid linked to amide group, respectively. The $–CH_2–NH–$ (50.41 ppm), $–CH_2–$ of citric acid (34.41 ppm) and $–CH_2–$ of aspartic acid (18.27 ppm) carbons are observed from ^{13}C NMR spectrum of PAC, which confirmed that the copolymer used in this study was PAC.

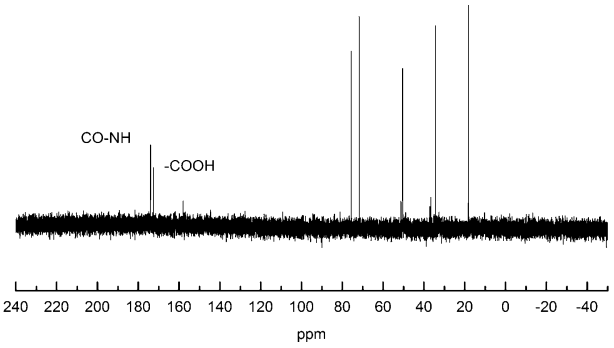

Fig. 2. ^{13}C NMR spectra of PAC.

^{1}H NMR spectra of PAC are shown as Fig. 3. The proton resonance peaks of –NH (–CO–NH), the methene ($–CH_2$) of citric acid and the methene ($–CH_2$) of aspartic acid are seen at the chemical shifts from 1.45–1.58 ppm, 2.06–2.13 ppm and 4.46–4.78 ppm, respectively. Shielding area appeared up and down direction of a double bond. The chemical shift of C=O is at 2.98–3.03 ppm in high magnetic field. 2.06–2.13 ppm and 4.46–4.78 ppm in the formant indicated that PAC copolymer existed isomer, which further indicates the structure of copolymer.

3.2. The proportions of PAC and HPMA in the blend

As shown in Fig. 4, the inhibition efficiency of PAC-HPMA changed with the variations of the proportions of PAC and HPMA in the blend. When the ratio of HPMA and PAC was 2:1, scale inhibition rate of PAC-HPMA was maximum value, which was able to 60.5%. Thus, the optimal proportions of HPMA and PAC are 2:1 in the blend of PAC-HPMA.

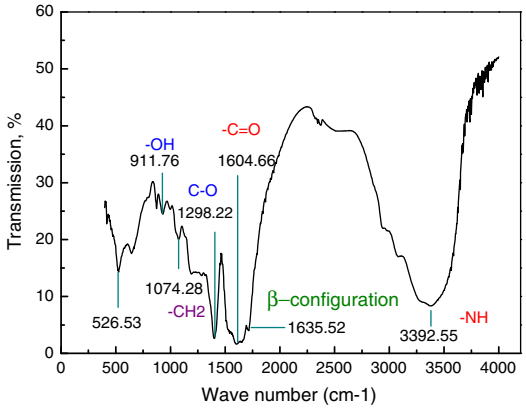

Fig. 1. FTIR spectra of the copolymer PAC.

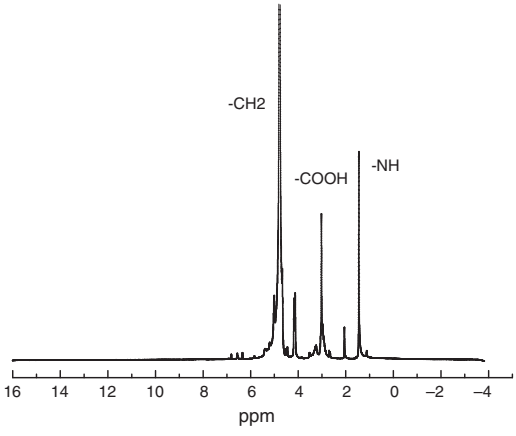

Fig. 3. ^{1}H NMR spectra of PAC.

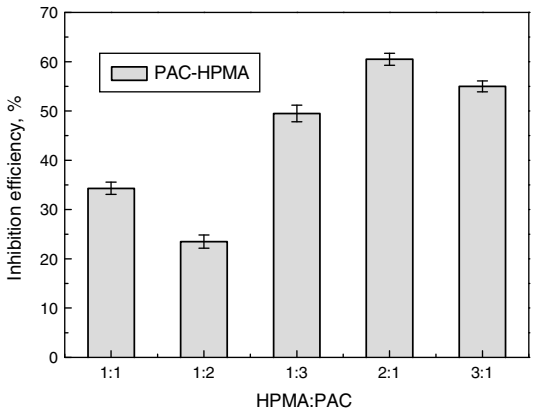

Fig. 4. The proportions of PAC and HPMA in the blend (C_{Ca}^{2+} = 100 mg/L, C_{PO4}^{3-} = 5 mg/L, pH = 9.0, T = 80 °C, and t = 10 h).

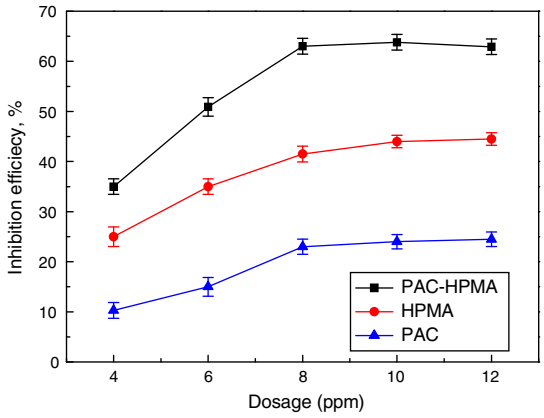

Fig. 5. Influences of inhibitor concentrations on inhibition rate (C_{Ca}^{2+} = 100 mg/L, C_{PO4}^{3-} = 5 mg/L, pH = 9.0, T = 80 °C, and t = 10 h).

3.3. Influences of inhibitor concentrations on inhibition rate

Fig. 5 shows the variations of inhibition rates of PAC-HPMA, HPMA and PAC against $Ca_3(PO_4)_2$ scale with the inhibitor concentrations. The inhibition on calcium phosphate scales substantially increased when the inhibitor dosages increased. The change might be interpreted as follows: after the scale inhibitor was added into the solution, chelating reactions between the carboxyl and scale ions (Ca^{2+} and Mg^{2+}) occurred in aqueous solution and scale inhibitor-Ca or scale inhibitor-Mg was adsorbed on the surface of scale crystal. The microcrystallines with the same charges repelled each other, prevented the formation of crystal nucleus, and reduced the growth rate of crystals. Moreover, microcrystallines could not form the normal scale, therefore preventing the formation of the scale. Thus, the scale inhibition rate increased. When the dosage of inhibitor was 8 mg/L, the scale-inhibiting rate on $Ca_3(PO_4)_2$ of PAC, HPMA and PAC-HPMA, respectively reached their peak values of 23%, 41.5% and 63%, and became stable when the dosage of inhibitor exceeded 8 mg/L. The inhibitor dosage showed the threshold effect (Garcia-Ramos & Carmona, 1982; Tjandra, Yao, Ravi, Tam, & Alamsjah, 2005). The phenomenon might be interpreted as follows. In the condition of pH 9.0, under the deprotonation effect, the carboxyl on the side chain of scale inhibitor molecules formed –COO^-, which reacted with calcium phosphate embryos, which existed in the solution, but had not yet formed crystals. Scale inhibitor molecules were adsorbed on the surface of calcium phosphate embryos and interacted with Ca^{2+} in the solution (Fig. 6A). If we continued to increase the dosage of scale inhibitor in the water system, inhibitor molecules adsorbed on the surface of the calcium phosphate embryos and Ca^{2+} also increased to the saturated states (Fig. 6B). The scale inhibitor dosage corresponding to the saturated state was the critical value, and excessive scale inhibitors added to the water system could not change its scale inhibition rate. The anti-scaling rate of PAC-HPMA was 63% higher than adding that of HPMA and PAC up because of the synergistic effect of HPMA and PAC.

3.4. Influences of concentration of Ca^{2+} on inhibition rate

Fig. 7 shows the influences of the concentration of Ca^{2+} on the scale inhibition rate. The scale inhibition rate decreased with the increasing concentration of calcium ions because the increase of calcium ion concentration facilitated the formation of the scale crystal, accelerated the crystallization process, and reduced the anti-scaling rate. Scale inhibition rate of PAC-HPMA was 35% higher than that of PAC and 20% higher than that of HPMA. When Ca^{2+} concentration was more than 150 mg/L, the inhibition rate of HPMA and PAC decreased rapidly and even declined to 50% or less. However, when Ca^{2+} concentration reached

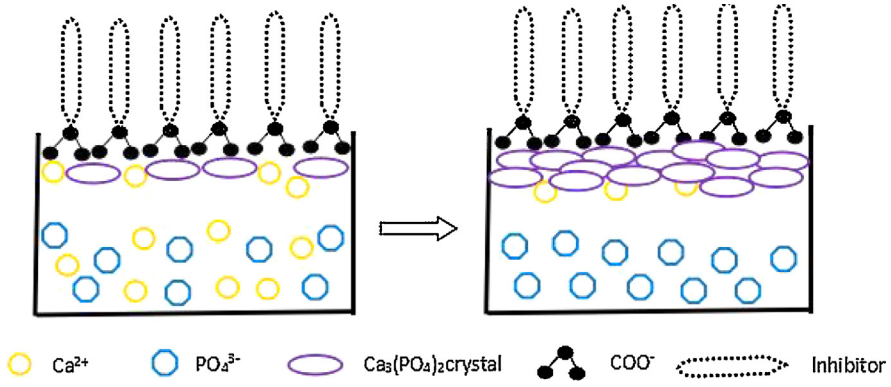

Fig. 6. Schematic diagram of the threshold effect.

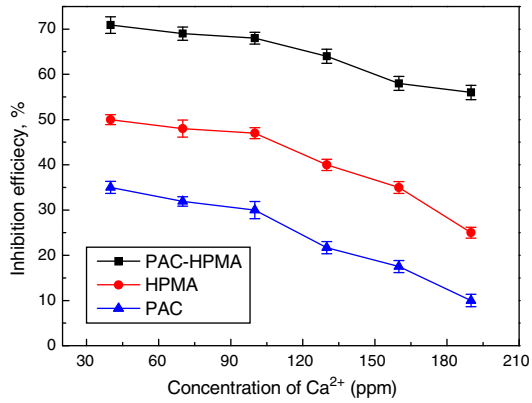

Fig. 7. Influences of the concentration of Ca^{2+} on inhibition rate (inhibitor concentration of 8 mg/L, $C_{PO4}{}^{3-}$ = 5 mg/L, pH = 9.0, T = 80 °C, and t = 10 h).

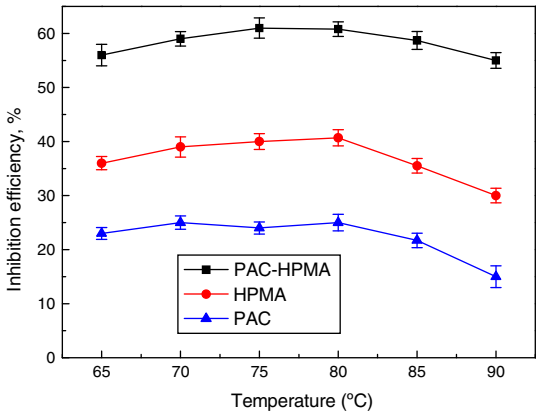

Fig. 9. Influences of temperature on inhibition rate ($C_{Ca}{}^{2+}$ = 100 mg/L, inhibitor concentration of 8 mg/L, $C_{PO4}{}^{3-}$ = 5 mg/L, pH = 9.0, and t = 10 h).

190 mg/L, the inhibition rate of PAC-HPMA was still maintained at 57.6%, which was only decreased by only 13.9% compared with the highest scale inhibition rate obtained under the Ca^{2+} concentration of 40 mg/L. This showed that PAC-HPMA still exhibited the satisfactory inhibition rate in high hardness water, which allowed the wider industrial application scope of the inhibitor.

3.5. Influences of pH on inhibition rate

Fig. 8 shows the influences of pH on the inhibition rates of PAC-HPMA, HPMA, and PAC against $Ca_3(PO_4)_2$ scale. With the pH rise, the inhibition rate firstly showed a slowly increasing trend because scale inhibitors were salts of weak acid, which were easier to dissociate and form anions under the alkaline condition and react with scale ions (Shakkthivel & Vasudevan, 2006). When the pH continued to increase, the inhibition rate gradually decreased, indicating that the growth rate of calcium phosphate crystals was far greater than the dissociation rate of scale inhibitors. Inhibition rate of PAC-HPMA was significantly higher than that of PAC and HPMA. The inhibition rate of PAC-HPMA was 20% higher than that of HPMA and 30.8% higher than that of PAC. The scale inhibition rate curve of PAC-HPMA showed a slow downward trend with the pH rise. At pH 11, its scale inhibition rate was still 60.2%. The results showed that compared with two kinds of monomers (PAC and HPMA), PAC-HPMA showed the higher alkaline tolerance and was more suitable in the high alkaline water conditions. The pH of general circulating cooling water systems was between 7 and 9.2. The compound agent (PAC-HPMA) could be used as the scale inhibitor in circulating cooling water systems.

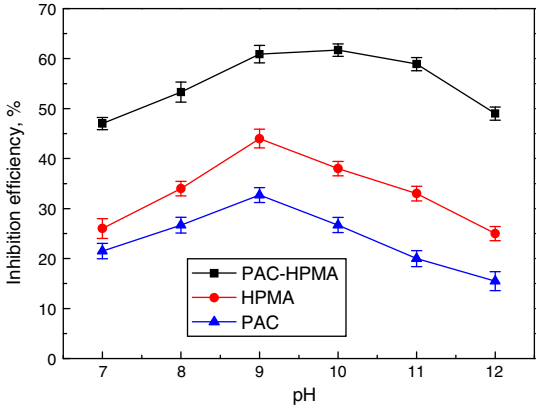

Fig. 8. Influences of pH on inhibition rate ($C_{Ca}{}^{2+}$ = 100 mg/L, inhibitor concentration of 8 mg/L, $C_{PO4}{}^{3-}$ = 5 mg/L, T = 80 °C, and t = 10 h).

3.6. Influence of temperature on inhibition rate

Fig. 9 shows the influences of temperature on the scale inhibition rate. When temperature was in the range of 65–80 °C, the inhibition rate remained steady with slight change. When the temperature rose above 80 °C, three inhibition rate curves showed a downward trend. The trend might be interpreted in two aspects. Firstly, with the temperature rise, crystal nucleus adsorption ability to scale inhibitor dropped and the desorption process was enhanced. Crystal growth rate was accelerated and crystals were gathered to form larger particles (Can & Üner, 2015; Rafieerad, Ashra, Mahmoodian, & Bushroa, 2015). Secondly, calcium phosphate had the abnormal solubility, which was reduced with the rise of temperature (Gao, Fan, Ward, & Liu, 2015). When the temperature rose to a certain value, calcium phosphate was in the supersaturated state, and finally precipitated. The inhibition rate of PAC-HPMA was about 34% higher than that of PAC and 20% higher than that of HPMA. The downward trend of inhibition rate curves of PAC and HPMA were more obvious with the temperature rise. When the temperature was 90 °C, the inhibition rates of PAC and HPMA were respectively 8.3% and 10.1% lower than their peak values. The scale inhibition rate curve of the PAC-HPMA showed a gentle downward trend, the scale inhibition rate at 90 °C was 56.0%, which was only 5.5% lower than the peak value of scale inhibition rate. In conclusion, PAC-HPMA exhibited better thermal resistance and could realize the satisfactory scale inhibition rate in the water systems with the large temperature variation change.

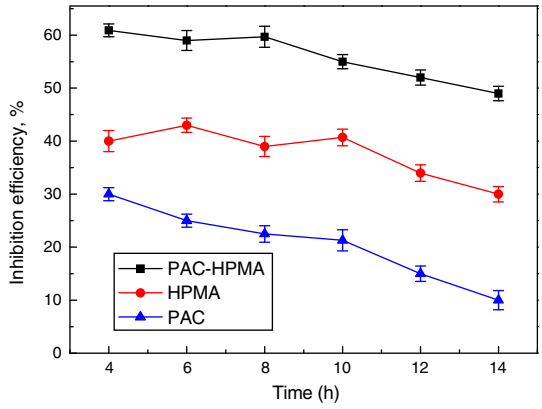

Fig. 10. Influences of treatment time on inhibition rate ($C_{Ca}{}^{2+}$ = 100 mg/L, inhibitor concentration of 8 mg/L, $C_{PO4}{}^{3-}$ = 5 mg/L, and pH = 9.0).

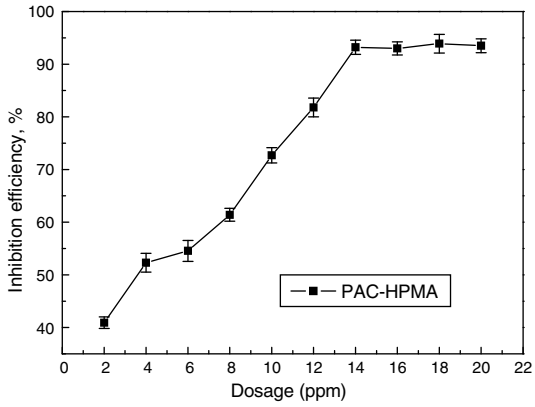

Fig. 11. Scale inhibition effect of compound inhibitor under the actual working condition ($C_{Ca}{}^{2+}$ = 100 mg/L, $C_{PO4}{}^{3-}$ = 1 mg/L, pH = 9.0, T = 80 °C, and t = 10 h).

3.7. Influences of treatment time on inhibition rate

Fig. 10 shows the influence of treatment time on the scale inhibition rate. With the increase in treatment time, the scale inhibition rate gradually decreased. When treatment time exceeded 10 h, the rate was decreased rapidly. It could be interpreted as follows. The scale inhibitor was adsorbed on the active surface of crystals so as to prevent or slow the growth rate of the crystal, thus leading to a long induction period (Al-Roomi & Hussain, 2014; Euvrard, Martinod, & Neville, 2011). Therefore, the anti-scaling rate was high before the treatment temperature time reached 10 h. However, after the induction period, the high temperature provided sufficient energy to molecules to overcome the activation energy of the reaction, and the crystal nucleus began to rapidly accumulate. Crystal grew up gradually and the scale in the solution was increased. Moreover, after the long treatment time, the inhibitor was gradually degraded and the adsorption quantity was decreased. Consequently, the anti-scaling rate of compound inhibitor PAC-HPMA was about 33.5% higher than that of PAC and 18.4% higher than that of HPMA. The scale inhibitor rate curve showed a declining trend. With the continuous increase in treatment time, the inhibition rate of PAC-HPMA decreased slowly. After 14 h, the scale rate was still 52.3%, which was only 9.4% lower than its peak value. While PAC monomer was used as scale inhibitor, with the increase in treatment time, scale inhibition rate decreased rapidly from 30% to 7.3%. The results showed that PAC-HPMA was applicable to in circulating cooling water system with the long hydraulic retention time.

3.8. Scale inhibition effect of compound inhibitor under the actual working conditions

The ability of PAC-HPMA to control calcium phosphate deposits is shown in Fig. 11. Under the actual working conditions of a circulating cooling water system, scale inhibition rate firstly increased with the increasing concentration of compound inhibitor and then leveled off. The results obtained with the Chinese national standard measurement method (GB/T 22626-2008) showed the same trend. PAC-HPMA displayed the superior ability to prevent the precipitation of calcium phosphate and its inhibition rate was approximately 100% at the dosage of 14 mg/L. In simulated actual working conditions, the anti-scaling rate of PAC-HPMA was excellent and fully met the actual application requirements of scale inhibitor in circulating cooling water systems. Hence the compound inhibitor can be used as an efficient "green" water treatment chemical against calcium phosphate precipitation.

3.9. Scale inhibition mechanism

The $Ca_3(PO_4)_2$ scale deposits were identified by AFM.

As shown in Fig. 12, in the absence of inhibitor, calcium phosphate particles showed the largest size and were overlapped each other (Fig. 12A). After the inhibitor PAC was added, the inhibitor obviously decreased the size of calcium phosphate solid particles, thereby dispersing them. However, partial scale particles were still overlapped (Fig. 12B). In the presence of HPMA-PAC scale inhibitors, scale particles became small without overlapping accumulation phenomenon and tended to be loose (Fig. 12C). According to the above data (Table 1), after PAC was added as scale inhibitor, the changes of each parameter of single scale particle were not obvious. The surface distance and the horizontal distance of single scale particle were respectively decreased by 18.9% and 22.8%, but the vertical distance remained unchanged. The PAC inhibition effect of calcium phosphate was generally not satisfactory. Similarly, when PAC-HPMA was used as scale inhibitor, the surface distance, the horizontal distance and the vertical distance of calcium phosphate particle size were obviously decreased by 75.6%, 77.0% and 52.0%, indicating that the scale-inhibiting effect was excellent. In the absence of the scale inhibitor, the gradient angle was

Table 1
Comparison of particles parameter by three kinds of inhibitors.

Inhibition parameters	Blank	PAC	PAC-HPMA
Surface distance (nm)	292.58	237.34	71.45
Horizontal distance (nm)	253.51	195.83	58.40
Vertical distance (nm)	62.52	73.55	30.04
Gradient angle (°)	13.85	20.59	27.22

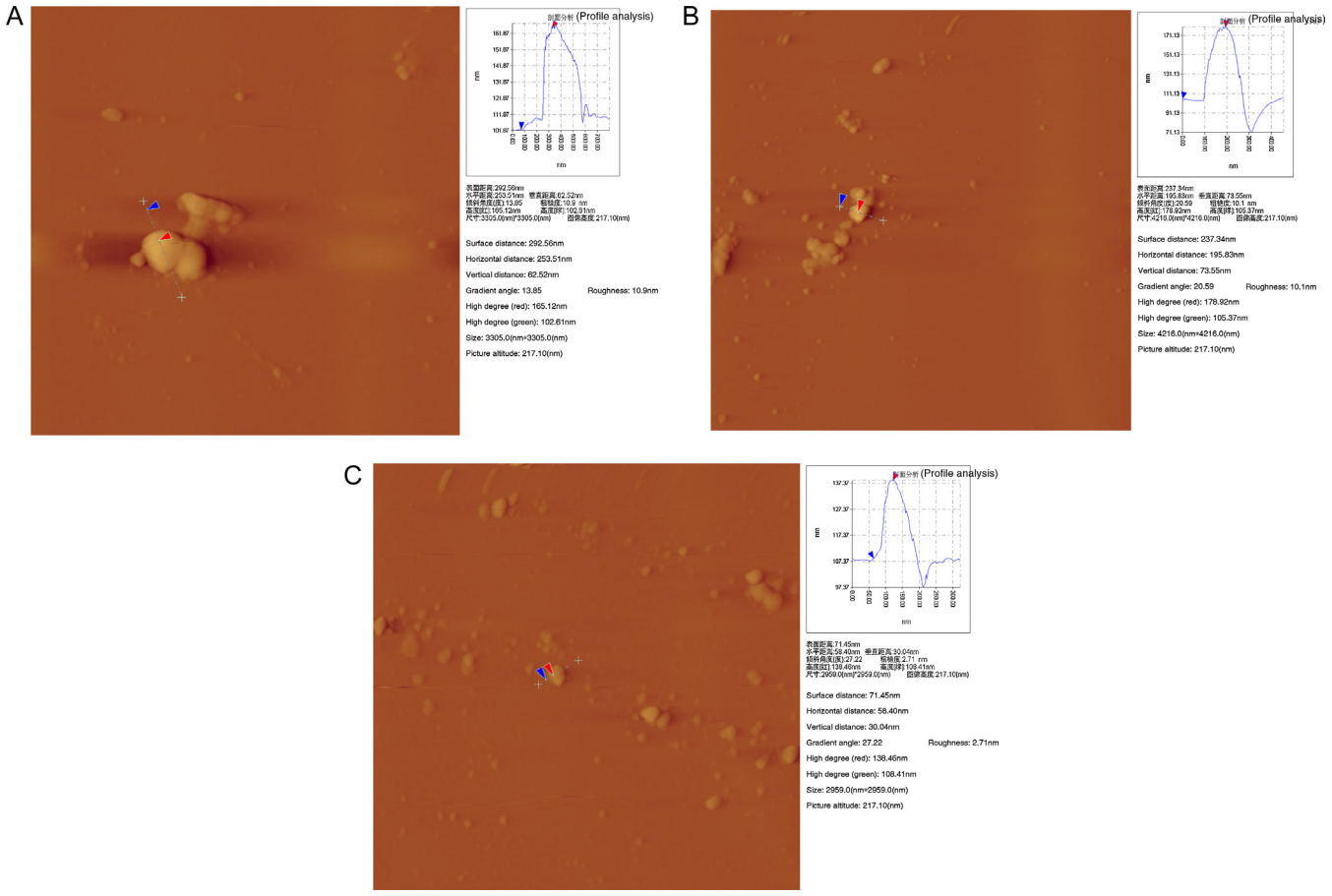

Fig. 12. AFM pictures of $Ca_3(PO_4)_2$ scale deposits obtained under 3 different conditions: (A) without scale inhibitor, (B) with PAC, and (C) with PAC-HPMA.

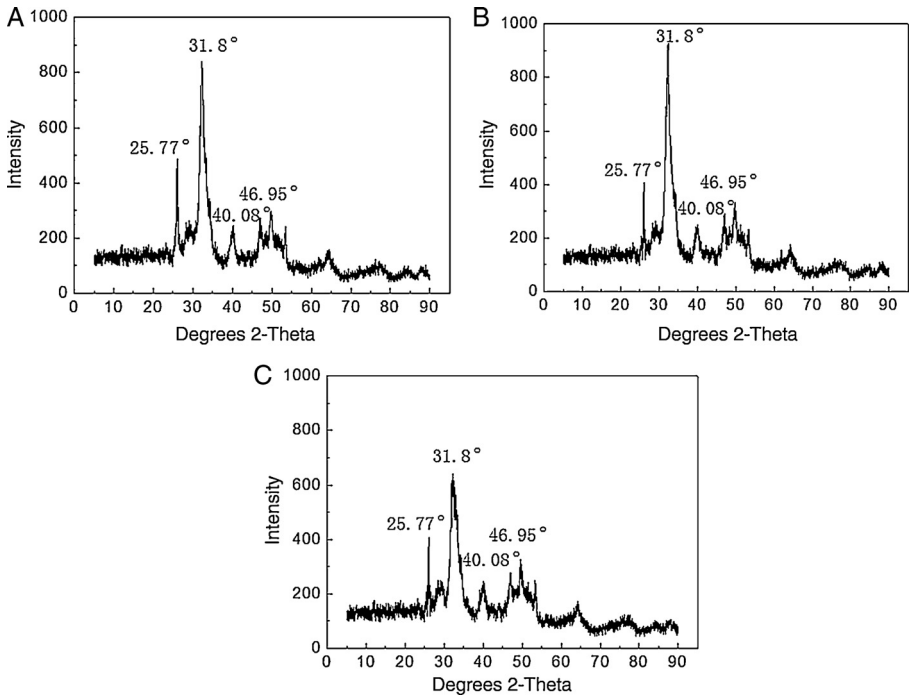

Fig. 13. XRD pattern of the $Ca_3(PO_4)_2$ crystals: (A) in the absence of inhibitor, (B) in the presence of PAC, and (C) in the presence of PAC-HPMA.

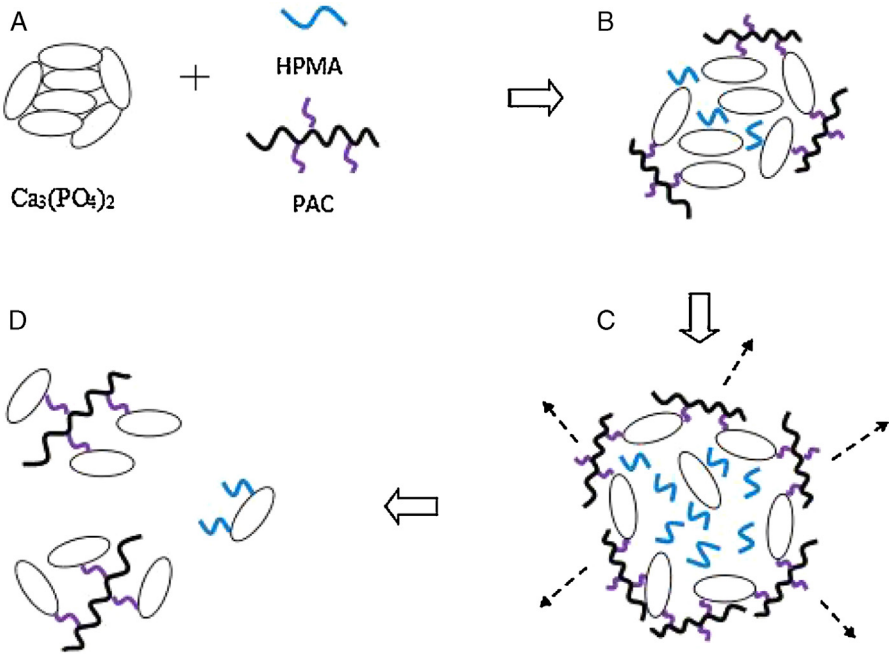

Fig. 14. Schematic diagram of the inhibition mechanism against $Ca_3(PO_4)_2$.

13.85; in the presence of PAC and PAC-HPMA, the gradient angles were, respectively, 20.59 and 27.22. The more irregular shape of scale particles indicated the better scale inhibition effect. AFM images indicated that the scale inhibitor achieved the scale inhibition efficiency by decreasing the calcium phosphate deposit size.

The precipitated phases were identified by XRD (Fig. 13). In the absence of the inhibitor, diffraction peaks of 25.77°, 31.8°, 40.08°and 46.95° in Fig. 13A, which are characteristic peaks of HAP crystals (Cai, Peng, Zi, Chen, & Qian, 2015), are extremely strong. After the addition of PAC and PAC-HPMA, these basic diffraction peaks do not change, but the relative intensities of the peaks become weak in Fig. 13B and tend to quite weak in Fig. 13C, indicating that the particle size decreases and makes the crystal structure loose (Lapwanit, Trakulsujaritchok, & Nongkhai, 2016; Wang et al., 2014).

In the circulating water system, because of the extremely low solubility of $Ca_3(PO_4)_2$, the main inhibition mechanism of PAC-HPMA against $Ca_3(PO_4)_2$ is realized through the dispersion effect rather than the chelating solubilization. The compound inhibitor was a blend of the low-molecular-weight polymer electrolyte (HPMA) and the long-chain polymer material (PAC) according to a certain proportion. Calcium phosphate scale was formed in the water because the solubility of calcium phosphate was small (Fig. 14A). After the compound inhibitor was added into water, HPMA entered into the cracks of the calcium phosphate scale. Because HPMA had the short-chain structure and low molecular weight. PAC containing lots of carboxyl groups could chelate with calcium ion and PAC as a long-chain macromolecule material was only adsorbed outside of the calcium phosphate. Therefore, the formed scales were loose (Fig. 14B). With the increase in HPMA, the cracks of calcium phosphate were more and bigger, and the scale became looser and stably chelated with a large number of PAC (Fig. 14C). Some calcium phosphate scales were bound with HPMA, and others were with PAC. Finally, they were completely dispersed in water (Fig. 14D).

4. Conclusions

As a novel “green” inhibitor, the scale inhibition rate of PAC against $Ca_3(PO_4)_2$ was about 23% under the dosage of 8 mg/L. However, the calcium phosphate inhibition rate of PAC-HPMA reached 63% under the limit dosage of 8 mg/L in the experiment, and the compound inhibitor showed a better inhibition rate than the two kinds of monomers (PAC and HPMA). Under the actual working condition, the inhibition rate of the compound inhibitor was close to 100% and completely met the actual application requirements of scale inhibitor in circulating cooling water systems. The compound inhibitor could be applied in circulating cooling water systems with the working conditions of high hardness, high temperature, and long hydraulic retention time.

FTIR analysis and ^{1}H NMR and ^{13}C NMR analysis confirmed the structure of PAC copolymer. Atomic force microscope (AFM), X-ray powder diffraction (XRD) analysis and scale formation process analysis showed that the copolymer of PAC affected the growth rate and the morphology of the calcium phosphate crystals and the influence of its compound inhibitor was more significant. The inhibition mechanism toward $Ca_3(PO_4)_2$ deposits was the decomposition-chelation dispersion effect.

Conflict of interest

The authors have no conflicts of interest to declare.

Acknowledgements

We thank all staff for AFM and XRD measurements. In addition, financial support from the NSFC (Natural Science Foundation of China, Grant No. 51308211), the Fundamental Research Funds for the Central Universities (Grant No. 2015MS63) and the Natural Science Foundation of Hebei Province are gratefully acknowledged.

References

Al-Roomi, Y. M., & Hussain, K. F. (2014). Antiscaling properties of novel maleic-anhydride copolymers prepared via iron (II)-chloride mediated ATRP. *Journal of Applied Polymer Science*, *131*, 221–229.

Belarbi, Z., Gamby, J., Makhloufi, L., Sotta, B., & Tribollet, B. (2014). Inhibition of calcium carbonate precipitation by aqueous extract of *Paronychia argentea*. *Journal of Crystal Growth*, *386*, 208–214.

Can, H. K., & Üner, G. (2015). Water-soluble anhydride containing alternating copolymers as scale inhibitors. *Desalination*, *355*, 225–232.

Cai, Z. Y., Peng, F., Zi, Y. P., Chen, F., & Qian, Q. R. (2015). Microwave-assisted hydrothermal rapid synthesis of calcium phosphates: Structural control and application in protein adsorption. *Nanomaterials*, *5*(3), 1284–1296.

Demadis, K. D., & Stathoulopoulou, A. (2006). Multifunctional, environmentally friendly additives for control of inorganic foulants in industrial water and process applications. *Materials Performance*, *45*(1), 40–44.

(2008). *Determination of scale inhibitor performance of water treatment agents—Calcium phosphate precipitation method*. Beijing: China Standards Press. GB/T 22626-2008.

Euvrard, M., Martinod, A., & Neville, A. (2011). Effects of carboxylic polyelectrolytes on the growth of calcium carbonate. *Journal of Crystal Growth*, *317*(1), 70–78.

Feng, J., Gao, L., Wen, R., Deng, Y., Wu, X., & Deng, S. (2014). Fluorescent polyaspartic acid with an enhanced inhibition performance against calcium phosphate. *Desalination*, *345*, 72–76.

Garcia-Ramos, J. V., & Carmona, P. (1982). The effect of some homopolymers on the crystallization of calcium phosphates. *Journal of Crystal Growth*, *57*(2), 336–342.

Gao, Y., Fan, L., Ward, L., & Liu, Z. (2015). Synthesis of polyaspartic acid derivative and evaluation of its corrosion and scale inhibition performance in seawater utilization. *Desalination*, *365*, 220–226.

Hasson, D., Shemer, H., & Sher, A. (2011). State of the art of friendly "green" scale control inhibitors: A review article. *Industrial & Engineering Chemistry Research*, *50*(12), 7601–7607.

Lin, Y. P., & Singer, P. C. (2005). Inhibition of calcite crystal growth by polyphosphates. *Water Research*, *39*(19), 4835–4843.

Liu, D., Dong, W., Li, F., Hui, F., & Lédion, J. (2012). Comparative performance of polyepoxysuccinic acid and polyaspartic acid on scaling inhibition by static and rapid controlled precipitation methods. *Desalination*, *304*, 1–10.

Lapwanit, S., Trakulsujaritchok, T., & Nongkhai, P. N. (2016). Chelating magnetic copolymer composite modified by click reaction for removal of heavy metal ions from aqueous solution. *Chemical Engineering Journal*, *289*, 286–295.

Roweton, S., Huang, S. J., & Swift, G. (1997). Poly (aspartic acid): Synthesis, biodegradation, and current applications. *Journal of Environmental Polymer Degradation*, *5*(3), 175–181.

Rafieerad, A. R., Ashra, M. R., Mahmoodian, R., & Bushroa, A. R. (2015). Surface characterization and corrosion behavior of calcium phosphate-base composite layer on titanium and its alloys via plasma electrolytic oxidation: A review paper. *Materials Science and Engineering: C*, *57*, 397–413.

Snoeyink, V. L., & Jenkins, D. (1980). *Water chemistry*. pp. 480. New York: Wiley.

Shakkthivel, P., & Vasudevan, T. (2006). Acrylic acid-diphenylamine sulphonic acid copolymer threshold inhibitor for sulphate and carbonate scales in cooling water systems. *Desalination*, *197*(1), 179–189.

Tjandra, W., Yao, J., Ravi, P., Tam, K. C., & Alamsjah, A. (2005). Nanotemplating of calcium phosphate using a double-hydrophilic block copolymer. *Chemistry of Materials*, *17*(19), 4865–4872.

Wang, C., Shen, T., Li, S., & Wang, X. (2014). Investigation of influence of low phosphorous co-polymer antiscalant on calcium sulfate dihydrate crystal morphologies. *Desalination*, *348*, 89–93.

Wang, J., Wang, D., & Hou, D. (2016). Hydroxyl carboxylate based non-phosphorus corrosion inhibition process for reclaimed water pipeline and downstream recirculating cooling water system. *Journal of Environmental Sciences*, *39*, 13–21.

Xu, Y., Zhang, B., Zhao, L., & Cui, Y. (2013). Synthesis of polyaspartic acid/5-aminoorotic acid graft copolymer and evaluation of its scale inhibition and corrosion inhibition performance. *Desalination*, *311*, 156–161.

Zuhl, R. W., & Amjad, Z. (2010). Scale and deposit control polymers for industrial water treatment. *Science and Technology of Industrial Water Treatment*, *6*, 81–103.

Zhang, H., Wang, F., Jin, X., & Zhu, Y. (2013). A botanical polysaccharide extracted from abandoned corn stalks: Modification and evaluation of its scale inhibition and dispersion performance. *Desalination*, *326*, 55–61.